Monatshefte für Chemie - Chemical Monthly (2023) 154:503–513
https://doi.org/10.1007/s00706-023-03057-4

ORIGINAL PAPER

Synthesis and characterization of polyacrylamide-based biomimetic underwater adhesives

Manuel Pühringer[1,2] · Christian Paulik[2] · Klaus Bretterbauer[2]

Received: 11 November 2022 / Accepted: 21 March 2023 / Published online: 12 April 2023

Abstract

Adhesion in an aqueous environment is still a challenging topic. In recent years, the focus on biomimetic adhesives inspired by mussel proteins has greatly increased. The present paper focuses on a straightforward synthesis route for three biomimetic polymers with opportunity in a multi-gram scale and an overall yield of 83% over three steps. Two synthesized monomers combined with commercially available monomers are the basis for three different co-polymers with varying catechol content with nature inspired concentrations. Catechol-bearing monomers were protected prior to polymerization. Tensile tests in dry or wet conditions were performed with the deprotected polymers. The measured adhesion values determined via tensile tests increase with the amount of catechol introduced in the polymers and the highest adhesion values of 2.0 MPa for underwater adhesion were found for poly(phenethyl acrylamide co dopamine acrylamide) co-polymers.

Graphical abstract

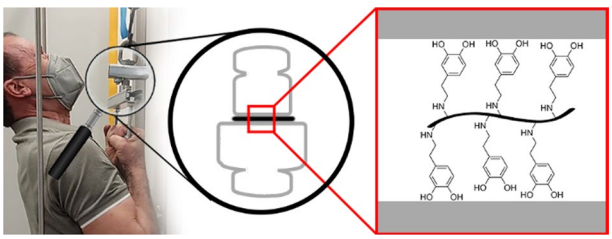

Keywords Adhesion · Biomimetic glue · Material science · Polymerization · Surface

Introduction

Mussel-inspired adhesion has become more and more prominent in biomimetic and biological science. The fascination with these sessile animals originates in their ability to adhere not only to rough mineral surfaces, but also to smooth surfaces such as marine paint, and this in aqueous environments [1]. Even on shore sites, these animals stay adhered despite waves reaching velocities of up to 25 m s^{-1} [2]. In contrast, man-made adhesives are challenged to adhere underwater with this amount of reliability [3]. In the last three centuries, research on unlocking the secret of this strong adhesion mechanism in an aqueous environment has grown enormously [4]. As more and more knowledge about the structure and composition of these adhesive threads excreted by the mussel is accumulated, imitation and clearer understanding have both increased. This is attributable to their ability to produce specific proteins from their ventral gap, the so-called byssus threads. These threads are between 30 and 40 mm in length and their ending spreads to up to 2 mm in diameter. Depending on the roughness of the environment, one single mussel excretes between 50 and 100 of these threads which are radially distributed around the ventral gap [4]. The outside of the thread consists of a large collagen protein, and the

✉ Klaus Bretterbauer
klaus.bretterbauer@jku.at

[1] CEST Centre for Electrochemistry and Surface Technology GmbH, Linz, Austria

[2] Institute for Chemical Technology of Organic Materials, Johannes Kepler University Linz, Linz, Austria

inside of the byssus, especially at the broad ending, consists of various smaller proteins, which are called mussel foot proteins (mfp) [5].

The two proteins mfp3 and mfp5 which are located closest to the surface contain the highest amount of L-3,4-dihydroxyphenylalanine (L-DOPA, Scheme 1) with values of 20% and 30%, respectively [4–6]. Ongoing research on how exactly this L-DOPA interacts not only with surfaces, but also with other amino acids such as lysine [7, 8] and histidine [9] are still to be intensified to really understand the mechanism. Although we still do not have a full understanding of this adhesion to surfaces underwater, researchers have already incorporated L-DOPA, or at least catechol-bearing motifs, into various materials such as self-healing hydrogels [10–12] or surgical wound closure materials [13], or to enhance wet adhesion performance [14–18]. Many reported materials are methacrylate based and find application primarily in the latter listed field [16–18]. Co-polymerization of methacrylates with acrylate-based monomers leads toward gradient polymers due to the much slower reactivity of methacrylate-based monomers [19]. To gain random implementation of the catechol-bearing monomers, only acrylate was used for a closer mimic of the random occurrence of L-DOPA within the mfp5 [4]. Furthermore, according to literature [20], high molecular weight polymers with a broad mass distribution is beneficial for the adhesive forces.

Herein, we focused on the synthesis of three different catechol functionalized polyacrylamides via free radical polymerization (FRP) technique to obtain a broad molar mass distribution and a corresponding high polydispersity index (PDI). Furthermore, the polymers are tested according to their adhesion to steel surfaces in dry and wet conditions.

Scheme 1

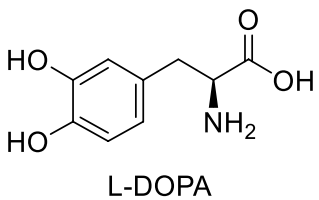

L-DOPA

Scheme 2

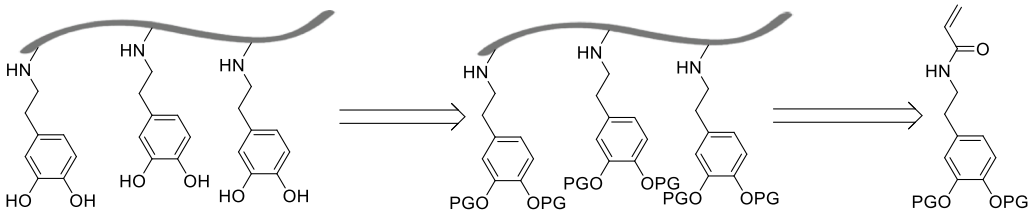

Results and discussion

Monomer synthesis

The preparation process, from monomer to adhesive polymer, should be achieved in a cost and time efficient synthesis pathway. Four monomers were used, where two of them were synthesized, and the other two purchased from standard suppliers. Concerning the catechol-bearing monomer, dopamine hydrochloride was chosen, as it constitutes a cost-efficient and readily available compound. Due to its nature of being a radical scavenger, the catechol group has to be O-protected prior to polymerization and afterward released from the polymer (Scheme 2). In the literature, various protecting groups (PG) are known, such as acetonide [21], methoxy [22], acetic esters [23], and silyl ethers [24]. The need to protect the amine functionality before the introduction of any of the first three PGs, due to its higher nucleophilic character, reduced the choice of a PG down to the latter due to the oxophilicity of Si. Comparing the stability and availability in cost-efficient amounts, the choice inclined toward *tert*-butyldimethylsilyl chloride (TBSCl) and trimethylsilyl chloride (TMSCl). However, trimethylsilyl-protected dopamine was found to decompose during the workup procedure. Additionally, TBSCl being solid made the synthesis procedure of the protecting step very simple and easy, as the used base, imidazole, was also a solid. Hence, all three components, dopamine hydrochloride, TBSCl, and imidazole, could be weighed into the same round bottom flask and the reaction was initiated by the addition of the solvent. The kinetics of this reaction furthermore increased the comfort of this procedure, as greater than 90% of all catechol groups were protected after merely 1 h of reaction time as determined by ^{1}H nuclear magnetic resonance (NMR) spectroscopy (Fig. S1, supplementary information). After 4 h, the reaction is quantitatively converted to 2-[3,4-bis[(*tert*-butyldimethylsilyl) oxy]phenyl]ethan-1-aminium chloride (**1**) (Scheme 3). The conversion and final product quality are confirmed with ^{1}H NMR spectroscopy (Fig. S2, supplementary information).

It is important to convert the amine into its hydrochloric salt **1**; otherwise, the product is not bench stable for longer than 1 day. In contrast, the protected dopamine

Scheme 3

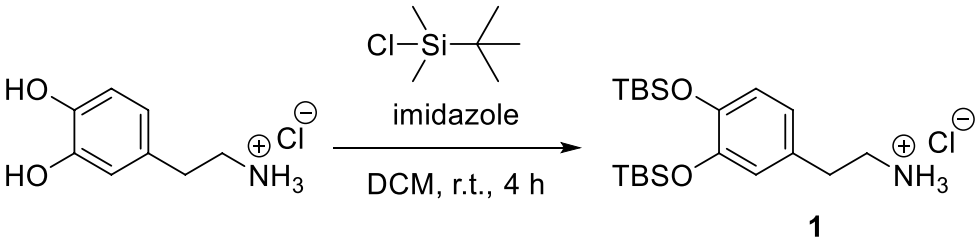

hydrochloride **1** is stable over months without any hints of degradation or side reactions as displayed in the comparison of the ^{1}H NMR spectra in Fig. S3 (supplementary information). After the introduction of the TBS groups into dopamine hydrochloride, **1** has then to be converted into a polymerizable monomer. This is accomplished by an acrylation reaction with acryloyl chloride using triethylamine (Et_3N) as base, yielding the key compound *N*-[2-[3,4-bis[[(1,1-dimethylethyl)dimethylsilyl]oxy]phenyl]ethyl]-2-propenamide (**2**) in 95% yield (Scheme 4). Figure S4 (supplementary information) shows the corresponding ^{1}H NMR spectrum.

Choosing methanol as a solvent for this reaction facilitates the workup, as the formed side product methyl acrylate originating from an excess of acryloyl chloride is simultaneously removed during the solvent removal process under vacuum. Only triethyl ammonium chloride and product **2** remain, which can be separated by a simple aqueous extraction. A one-pot synthesis starting from dopamine hydrochloride was attempted, but choosing imidazole as base during the protection step is essential to the fast and full conversion in contrast to Et_3N, whereas during the acryloyl chloride reaction step, the imidazole would also react with acryloyl chloride producing *N*-acrylimidazole as side product requiring column chromatography for separation and drastically decreasing the yield of **2**. Thus, the key compound **2** could be synthesized in more than 85% after two steps, making the production of a monomer containing a catechol moiety an efficient process with an uncomplicated workup. Furthermore, without the need for column chromatography, this convenient synthesis route is also up-scalable to a multi-gram scale.

Polymer synthesis

The next step was the development of a tailored polymerization protocol providing a polymer with a molecular mass distribution for adhesion applications. The need for highly pure educts and water-free solvents renders the anionic polymerization technique unsuitable and a radical based polymerization was chosen instead. Here, the two controlled radical polymerizations, atom transfer radical polymerization (ATRP) and reversible addition – fragmentation chain-transfer polymerization (RAFT), or the simple free radical polymerization (FRP), are available. The former two techniques can produce polymers with a rather narrow PDI, whereas the latter yields a broad PDI. Imitating nature would mean producing polymers with highly narrow PDI, due to the fact that the proteins of the mussel each have one defined molecular weight. This was already tried in the group of J. Wilker [20], where anionic polymerization of styrene and 3,4-dimethoxystyrene was performed and the adhesive properties were compared between different molecular weights, and also a blend of their polymers with different sizes was examined. The result of this study was that the blend of small and big polymers was better due to the fact that the short polymer chains increase the adhesive features, whereas the high molecular weight fraction increases cohesion within the adhesive layer. Thus, the FRP technique was the method of choice because it normally produced a broad PDI. Another huge benefit is the straightforward preparation. There is no need for water-free solvents, some FRPs even being performed in water, but oxygen has to be removed. The two most applied methods are on the one hand the freeze-thawing method and on the other hand, bubbling argon or nitrogen through the solvent for at least 15 min. The requirements for the polymerization of **2** are

Scheme 4

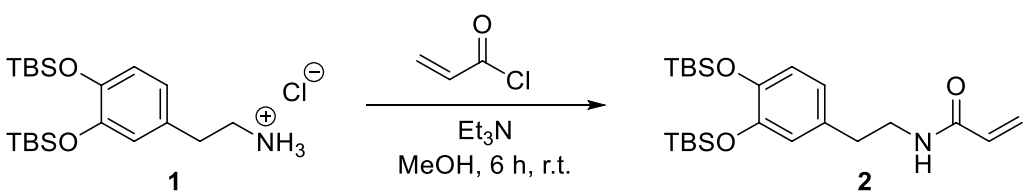

fulfilled by flushing the solvent with nitrogen and the FRP is performed under an argon atmosphere.

Acrylamide **2** was co-polymerized with butyl acrylate (BA) forming P(BA–TDAXX) (Fig. S5, supplementary information), methyl acrylate (MA) forming P(MA–TDAXX) (Fig. S6), or *N*-(2-phenylethyl)acrylamide (**3**, PAA) forming P(PAA–TDAXX) (Fig. S7), where XX depicts the amount of **2** introduced in the polymers in the range of 1–30% (Scheme 5). Benzene and *N*,*N*-dimethylformamide (DMF) were used as solvents for the synthesis of butyl acrylate co-polymers P(BA–TDAXX). The former was chosen for P(MA–TDAXX) and P(PAA–TDAXX) after screening for the best polymerization condition as described below. Benzene was chosen as an apolar solvent known to have a negligible effect on the polymerization of acrylates, implying limited interaction with the radicals formed, while DMF was chosen as a polar solvent for comparison [25]. Furthermore, toluene and 1,4-dioxane were tested as polymerization solvents, but afforded lower yields and higher residual monomer content and, therefore, the use of these solvents was refrained. Edeleva et al. [26] calculated that higher temperatures lead to higher side reactions such as backbiting or β-scission and that lower temperatures lead to rather large polymers. Furthermore, according to Ref. [20, 27], there is a breakeven point in the range of 80 kDa for polymers with a low PDI to increase adhesive force. Visually observable precipitation during the polymerization in DMF showed a size-controlled solubility of the polymer that could be confirmed by gel permeation chromatography (GPC) measurements obtaining M_w values in the range of 75–82 kDa. Figure 1 shows the GPC chromatogram of the produced polymers P(BA–TDA20) in benzene and DMF.

GPC revealed molecular weights M_w of 190 kDa for the synthesis in benzene, whereas synthesis in DMF reached 82 kDa. Therefore, polymerizations were performed in benzene, allowing to go toward higher M_w than in DMF. Additionally, in benzene more side reactions such as β-scissions are to be expected, leading to an increase of cohesion [26]. In the next step, the polymerization time has to be determined,

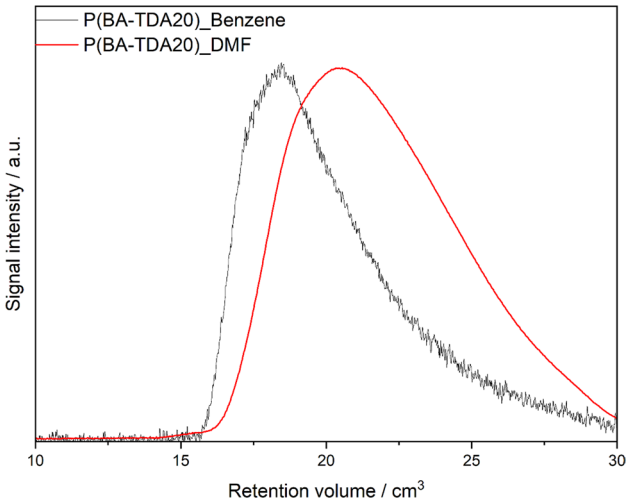

Fig. 1 GPC chromatogram of two synthesized polymers P(BA–TDA20) with 20% of the catechol-bearing monomer. Reaction carried out in benzene (black) with a molecular weight M_w greater than 190 kDa. In comparison, the reaction carried out in DMF (red) with a molecular weight M_w of 82 kDa (Color figure online)

Scheme 5

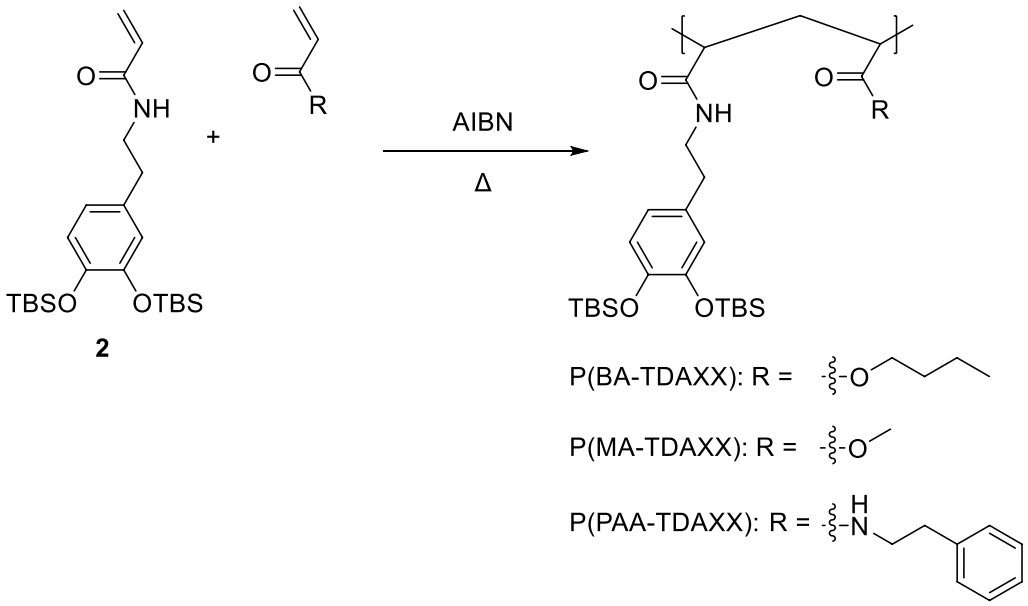

Table 1 Change in molecular weight during the reaction process of a P(BA–TDA20) sample

Time/min	M_w/kDa	M_n/kDa	PDI
15	241.860	105.800	2.28
30	215.450	83.200	2.58
60	204.700	66.500	3.07
120	194.970	54.800	3.55
180	199.500	54.900	3.63
240	191.800	49.400	3.88

Table 2 Molecular weights and PDI for P(BA–TDA20) synthesized in different monomer concentrations

Concentration	M_w/kDa	M_n/kDa	PDI
c_1	49.500	25.700	1.93
c_2	69.200	34.600	2.00
c_3	113.660	34.800	3.27
c_4	191.040	49.300	3.88

after which the synthesis can be quenched. Thus, samples were drawn after 15, 30, 60, 120, 180, and 240 min reaction time and analyzed with GPC. Table 1 shows the change in molecular weight over time for P(BA–TDA20) polymerization.

In the first 2 h, the molecular weight changes rapidly and a steady broadening of the PDI can be observed. After 2 h, the molecular weight as well as the PDI stays rather constant. The decrease in molecular weight over time can be explained by the occurrence of a variety of side reactions dominated by β-scissions according to Ref. [26]. To ensure a high molecular weight and a broad PDI, the reaction time was set to 4 h. In the next step, the control over the molecular weight via the concentration of the monomer solution was investigated. Thus, polymers were synthesized in four different concentrations. Hereby, **2** and butyl acrylate were placed together in a round bottom flask and dissolved in benzene in the total concentrations of 0.7 mmol cm^{-3} (c_1), 1.0 mmol cm^{-3} (c_2), 1.5 mmol cm^{-3} (c_3), and 2.0 mmol cm^{-3} (c_4). Table 2 lists the achieved GPC values for each concentration for the synthesis of P(BA–TDA20) with 2 mol% of AIBN as the initiator with respect to the combined monomer amount ([**2** + BA]:[AIBN] = 100:2).

The lowest two concentrations (Table 2, c_1 and c_2) result in polymers below the 80 kDa threshold for M_w [20]. Concentrations of 1.5 mmol cm^{-3} and above obtained polymers with suitable molecular weight and PDI for adhesive applications. Furthermore, residual free amine **1** does not interfere during the polymerization process and was separated along with unreacted monomer **2** and co-monomer butyl acrylate during the precipitation process of the polymer in cold methanol (MeOH). For precipitation, the concentration of the polymer solution is a key element. Concentrations greater than 2 mmol cm^{-3} result in droplets with solidified outer shell and with the insides containing still unpurified polymer solution, whereas a too-high dilution leads to a low or no precipitation of the polymer. The latter was also observed at the two higher diluted concentrations (Table 2, c_1 and c_2). Light fog formation during precipitation was observed for concentration c_2. The higher concentrations (Table 2, c_3 and c_4) both show good precipitation. While polymerization concentration c_3 is absolutely free from monomers after one single precipitation, the highest concentration c_4 still shows some slight presence of monomers according to ^{1}H NMR spectroscopy (Fig. 2). Therefore, the concentration for the following synthesis of polymers P(MA–TDAXX) and P(PAA–TDAXX) was set to 1.5 mmol cm^{-3}.

Analysis with differential scanning calorimetry (DSC) revealed that the glass-transition temperature (T_g) for the BA co-polymers is situated at − 9 °C, which is expectedly higher than the T_g of a BA-homopolymer at − 54 °C [28]. As the ideal value for a polymer applied in adhesion applications should be at least above room temperature, the co-monomer was changed from butyl acrylate to methyl acrylate [29]. Co-polymers P(MA–TDA20) and P(MA–TDA30) produced with this monomer reached a T_g of 39 °C and 45 °C, respectively, which was significantly higher than the ones with BA, but surprisingly showed weaker adhesion force discussed in the tensile testing section. Looking at the difference between the T_g values of polyacrylates and polyacrylamides, it is expected that the incorporation of acrylamides leads to an increase in the T_g [30]. Therefore, co-monomer **3** was synthesized in a single step to not only introduce another acrylamide, but also another aromatic moiety to also increase π-interactions with surfaces. Similarly to the synthesis of **2**, phenethylamine was dissolved in methanol and converted into the corresponding acryl amide **3** in 89% yield (Scheme 6). The conversion and final product quality were confirmed with ^{1}H NMR (Fig. S8, supplementary information).

Aqueous workup renders the monomer **3** directly insertable to polymerization and, comparably to polymerizations with **2**, the unreacted free amine precursor is separated during the precipitation step of the polymer P(PAA–TDAXX). This co-polymer reaches a T_g value of 85 °C as depicted in Fig. 3 (black line).

Deprotection and preparation for tensile testing

All polymers were deprotected directly before adhesion measurements due to the nature of the catechol moiety to oxidize under air, yielding a highly reactive *o*-chinone which shows cross-linking ability [31–33]. *O*-TBS

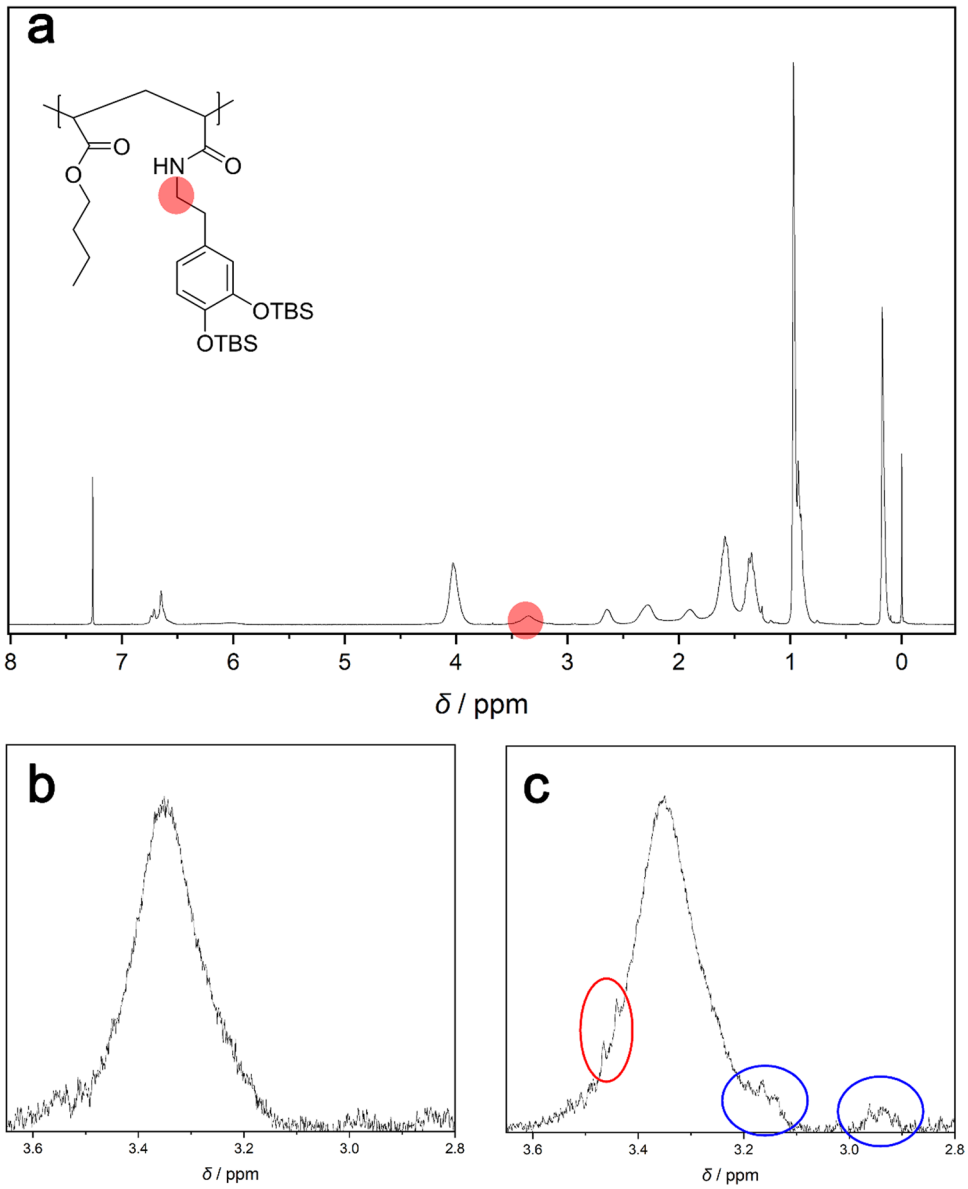

Fig. 2 ^{1}H NMR spectra of P(BA–TDA20) for determination of the concentration-dependent degree of purification. Samples were precipitated in cold MeOH. ^{1}H NMR spectrum of P(BA–TDA20) with highlight on the zoomed-in area and the corresponding hydrogens marked on the molecule scheme (**a**). Zoomed-in area for concentration c_3 showing no residual monomer signals after a single precipitation step (**b**) and concentration c_4 highlighting defined signals of unreacted monomer **2** (red circle) and signals of unseparated **1** (blue circles) (**c**) (Color figure online)

Scheme 6

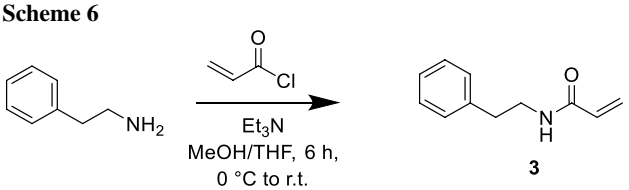

cleavage is achieved with the addition of a tetrabutylammonium fluoride (TBAF) solution in tetrahydrofuran (THF) [34]. Due to Si being highly fluorophilic, the deprotection is completed in just 30 min of reaction time at room temperature. The excess of TBAF as well as the by-products are separated from the polymer by precipitation in a cold MeOH/water (2:1) mixture, which is acidified with HCl to a pH below 3 to prevent the oxidation of the catechol moiety to the corresponding catecho-*o*-quinone. Figure 3 shows that the deprotection even increases the T_g value of P(PAA–TDA20) from 85 °C to 94 °C.

Furthermore, two polymers without the catechol moiety were synthesized for reference adhesion values. On the one hand, a co-polymer consisting of butyl acrylate and 20 mol% **3**, P(BA-PAA20), as an equivalent to P(BA–TDA20), and on the other hand, a homopolymer of **3**, P(PAA) were synthesized for comparison with P(PAA–TDAXX) polymers. ^{1}H NMR spectra for deprotected and catechol-free polymers are found in the supplementary information (Fig. S9–S13).

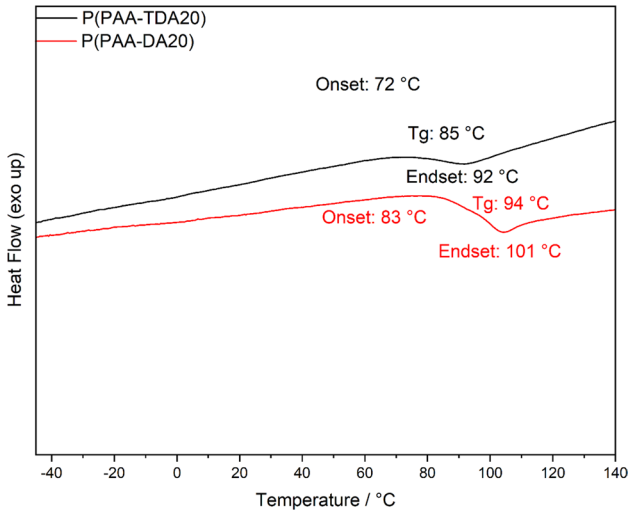

Fig. 3 DSC thermogram of the protected co-polymer P(PAA–TDA20) (black line) and unprotected P(PAA–DA20) (red line). Deprotection leads to a T_g-increase of about 10 °C (Color figure online)

Tensile testing

For the preparation of tensile tests, a stamp set of two different sized stamps was used. One stamp had a diameter of 30 mm and the other a diameter of 20 mm. This design enables an easy application, even under water, of the polymer solution onto the bigger stamp and comprehensive adhesive coating of the thereafter applied smaller stamp. The adhesive force is calculated for the diameter of the smaller stamp.

Prior to the application of the polymer solution, all stamps were cleaned and degreased, twice in THF, twice in acetone, and twice in 2-propanol (*i*PrOH) in an ultrasonic bath for 15 min each. All polymers were dissolved in a mixture of chloroform ($CHCl_3$) and MeOH (9:1) in a concentration of 300 mg cm^{-3} [35]. Via an Eppendorf syringe, 100 mm^3 of polymer solution is applied onto the bigger stamp in a circle, which was roughly the size of the smaller stamp (Fig. 4). The reason for choosing $CHCl_3$ as the main component in the solvent mixture was for the underwater application of the polymer solution. The stamp was already immersed in artificial seawater, the solution was applied under water, and with the higher density of $CHCl_3$ the film remained underwater. Methanol was added as a solubilizer, allowing the polymer to solidify and fully precipitate underwater in the course of 24 h. Figure 4 shows the applied film underwater in a top view (Fig. 4a), side view (Fig. 4b), and with the applied smaller stamp (Fig. 4c).

In literature, adhesion values are often gained using aluminum or sanded steel via leap shear force measurements making it harder to really compare these values with those gained in this work. Nevertheless, the values presented

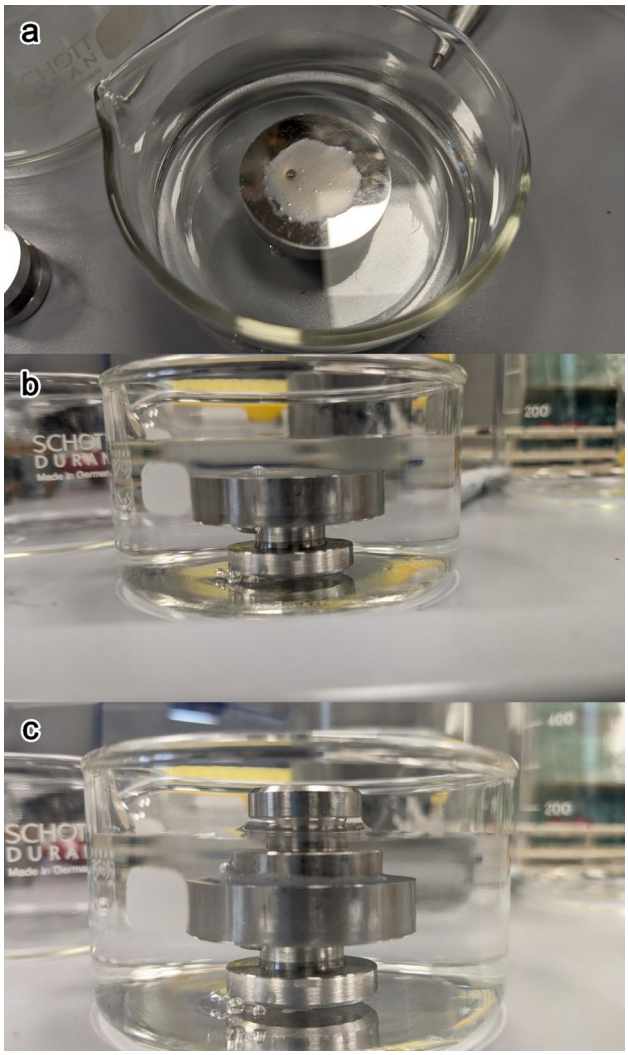

Fig. 4 Picture of the applied polymer layer P(BA–DA20) on a stamp already immersed in artificial seawater top view (**a**) and from the side (**b**). A side view after covering the polymer layer with the smaller stamp to let it cure overnight at room temperature while kept under water (**c**)

here are obtained under harder conditions, as the steel is not sanded but polished reducing the surface area and gaps the adherent is applied onto. Furthermore, the pull-off tests performed in this work represent the worst case for the adhesion layer as the force is normal to the layer in contrast to the leap shear force analysis where the force is along the adhesion layer. Having this in mind, values found in the literature range from 2.6 MPa and 1.0 MPa in dry and wet conditions, respectively, after additional cross-linking via IO_4^- oxidation [36] and 1.1 MPa under wet and dry conditions on aluminum surfaces [37]. The addition of a phosphate motif increases the adhesion

values to around 2.5 MPa after IO_4^- crosslinking in dry conditions and 0.5 MPa in wet conditions [38].

For all different polymers, the tensile test results are listed in Table 3. Dry adhesion values were obtained after drying at room temperature for 24 h, or after drying for 1 h at room temperature, then putting the stamps into a drying oven at 60 °C for 22 h, and removing them 1 h prior to tensile testing. This temperature was chosen as it was slightly underneath both boiling points of the solvents used for the application of the polymers on the stamps. Wet adhesion values were obtained after drying underwater for 24 h and subsequent removal from the aqueous medium just before the tensile tests.

Tensile testing revealed that the adhesion force correlates with the amount of catechol introduced into the polymer for all biomimetic co-polymers except for P(BA–DA30). The generally low adhesion forces for P(BA–DA30) are attributed to wetting problems during the application of the adhesive layer. Furthermore, the BA-co-polymers P(BA–DAXX) are honey-like at room temperature, leading to thread formation and weak adhesion forces during tensile testing (Fig. S14, supplementary information). As expected, both polymers without the catechol moiety (P(BA-PAA20) and P(PAA), Table 3) showed lower adhesion forces compared to the corresponding biomimetic polymers, except for the homopolymer P(PAA) after curing at 60 °C. A possible reason is seen in the combination of a lower T_g (79 °C) and especially the broader PDI (3.72 vs. 3.03), resulting in a higher content of short polymer chains providing a better surface wetting during the curing process. There is also a significant increase in adhesion force when the curing temperature is increased to 60 °C. This is attributed to the faster and better withdrawal of the solvent mixture and therefore a better surface wetting of P(BA–DAXX). P(PAA–DA10) and P(PAA–DA20) show no significant increase in adhesion force when cured at 60 °C, most probably due to no change in 3D polymer structure as their T_g values of 84 °C and 94 °C, respectively, are not exceeded. Underwater tests showed a similar trend. With an increased amount of catechol higher adhesion forces are obtained. Despite very low adhesion forces for P(MA–DAXX) polymers, this trend still is observable. In contrast, P(PAA–DAXX) polymers showed the best underwater adhesion forces affording 2 MPa at 20% catechol content and therefore more than doubled the adhesion force compared to the corresponding homopolymer P(PAA). Additionally, P(PAA–DAXX) shows an increase in adhesion force when immersed and cured in an aqueous environment compared to dry adhesion.

Table 3 Adhesion forces F measured for all synthesized co-polymers

Co-polymer	Dry, F_{rt}/MPa	Dry, F_{60}/MPa	Wet, F_{wet}/MPa
P(BA–DA1)	6.4×10^{-3}	1.0	0.60
P(BA–DA10)	0.10	2.4	0.85
P(BA–DA20)	0.65	3.2	0.95
P(BA–DA30)	0.40	3.4	0.45
P(MA–DA20)	1.2	–[a]	7.3×10^{-3}
P(MA–DA30)	2.4	–[a]	0.02
P(PAA–DA10)	1.2	1.3	1.8
P(PAA–DA20)	1.5	1.5	2.0
P(BA–PAA20)	0.33	1.1	0.55
P(PAA)	0.43	2.3	0.9

F_{rt} stands for drying at room temperature, F_{60} for drying at 60 °C, and F_{wet} for drying under water

[a]Adhesion layer failed during insertion into the sample mounting

Conclusion

Herein, we present a straightforward synthesis procedure for the bioinspired catechol-containing co-polymers P(BA–TDAXX), P(MA–TDAXX), and P(PAA–TDAXX), and their monomers **2** and **3**. Monomer synthesis is performed in two steps and with high conversion in both steps (90% for the first and 95% for the second), making it an attractive route with an 85% overall yield of isolated product. The developed syntheses allow a multi-gram scale production of the final polymers. Additional advantages are the use of low-cost chemicals with high-volume availability and convenient purification processes with no need for column chromatography. All polymers showed adhesive properties for curing under dry conditions. Outstandingly, P(PAA–DAXX) showed increased adhesion forces under aqueous conditions compared to values measured under dry conditions, especially in relation to values found in literature [36–38]. All synthesized polymers containing a catechol moiety showed an increase in adhesion force compared to their corresponding polymer without the catechol moiety, confirming the impact of this structure in adhesion mechanism.

Experimental

All reagents and solvents were purchased from commercial suppliers (Sigma-Aldrich, VWR, TCI) and were used without further purification. Unless stated otherwise, all reactions were carried out under an argon atmosphere. Artificial seawater was produced according to Ref. [39].

^{1}H and ^{13}C NMR spectra were recorded using a Bruker 300 MHz Avance III spectrometer. Chemical shifts (δ) are reported relative to tetramethylsilane (TMS) and were referenced to the residual signal of the deuterated solvent ($CDCl_3$: 7.26 ppm for ^{1}H and 77.16 ppm for ^{13}C NMR;

DMSO-d_6: 2.50 ppm for ^{1}H and 39.52 ppm for ^{13}C). The following abbreviations are used to describe observed multiplicity: s = singlet, s_{br} = broad singlet, d = doublet, t = triplet, and m = multiplet.

HPLC–MS analysis was performed by reversed-phase chromatography using a Surveyor HPLC (Thermo Fisher Scientific) equipped with a Zorbax SB-C18 column (150 mm × 2.1 mm i.d., 5 µm particle size; Agilent). The column temperature was set to 40 °C and the injection volume was 1 mm^3. Analytes were separated by gradient elution with mobile phase A containing 0.1% formic acid (FA) in water and mobile phase B containing 0.1% FA in acetonitrile at a flow rate of 0.2 cm^3 min^{-1}. The elution gradient starting conditions were 90% A and 10% B. After 1 min the proportion of B was increased to 95% at 25 min, where it was held for further 35 min.

High-resolution mass spectra were obtained using an LTQ Orbitrap Velios (Thermo Fisher Scientifc) with an APCI source operated in positive ionization mode. The resolution was set to 30.000 and diisooctylphthalate (m/z = 391.2843) was used as internal standard for mass calibration. Spectra were collected from 80 to 1.000 m/z and data were analyzed using Xcalibur (Thermo Fisher Scientific; version 2.2 SP1.48).

Molceular weights of the polymers were determined by GPC using an Agilent Technologies 1200 connected to an Agilent 1200 binary pump, three Phenogel columns (5 µm, 10^5 Å, 10^4 Å, 10^3 Å), a PL-ELS 1000 detector, and a Waters 410 Differential Refractometer detector. Polystyrene standards were purchased from Agilent and used for calibration.

DSC measurements were performed on a Mettler Toledo DSC 3 + STAR System with a heat–cool–heat run (− 40 °C to 140 °C at 10 °C min^{-1}) under constant nitrogen flow of 20 cm^3 min^{-1}. Glass-transition temperatures (T_g) were obtained from the second run of each sample.

All stamps, except for two stamp sets, were each sanded for 2 min first with a 220-grade paper, then with a 1000-grade paper, followed by a 2500-grade paper and finally polished with a 4000-grade paper. Tensile tests were performed with a Zwick Roell Type 8406 with a maximum force of 50 kN according to DIN EN ISO 4524. Test speed was 10 mm min^{-1} and the area used for calculation was fixed at 20 mm in diameter. Polymers were dissolved in $CHCl_3$:MeOH (9:1) in a concentration of 300 g dm^{-3} and 100 mm^3 were applied on each big stamp prior to being covered with the small stamp after 30 s of pre-drying time. Stamp sets were then dried 24 h in either wet conditions under artificial seawater, or 24 h under dry conditions at room temperature, or at room temperature for 1 h, then put in a drying oven at 60 °C for 22 h and removed 1 h prior to measurement to cool to room temperature again.

2-[3,4-Bis[(*tert*-butyldimethylsilyl)oxy]phenyl]ethan-1-aminium chloride (1, $C_{20}H_{40}ClNO_2Si_2$) Modified from Ref. [24]. Dopamine hydrochloride (10 g, 52.73 mmol), imidazole (4.0 eq., 210.92 mmol), and *tert*-butylchlorodimethylsilane (2.1 eq., 110.73 mmol) were weighed in a three-necked round bottom flask. 120 cm^3 of dichloromethane (DCM) were added to the reaction and the suspension was stirred at room temperature. After 4 h, the formed precipitation was filtered off and the filtrate was extracted two times with 10% sodium carbonate solution followed by twice extraction with 1% hydrochloric acid solution forming the hydrochloride salt of the amine and finally extracting once with brine. The organic layer was dried over sodium sulfate, the solvent was evaporated and the pale-yellow, almost white solid was used in the next step without further purification. Yield: 21.2 g of crude product (94% purity = > 90.3% yield of **1**); HRMS: m/z calculated for $[C_{20}H_{40}NO_2Si_2]^+$ ($[M+H]^+$) 382.2592, found 382.2592; ^{1}H NMR (300 MHz, $CDCl_3$): δ = 8.35 (3H, s, N**H$_3$**), 6.79–6.63 (3H, m, Ar–**H**), 3.17 (2H, s_{br}, Ar–C**H$_2$**–CH_2–NH_3), 2.98 (2H, dd, J = 10.3, 6.0 Hz, Ar–CH_2–C**H$_2$**–NH_3), 0.96 (18H, d, J = 0.9 Hz, Si–C–(C**H$_3$**)$_3$), 0.17 (12H, s, Si–(C**H$_3$**)$_2$) ppm; ^{13}C NMR (75 MHz, $CDCl_3$): δ = 146.7, 145.3, 132.5, 121.7, 120.9, 43.4, 38.8, 25.9, 25.7, 18.4, − 3.5, − 4.1 ppm.

***N*-[2-[3,4-Bis[[(1,1-dimethylethyl)dimethylsilyl]oxy]phenyl]ethyl]-2-propenamide (2, $C_{23}H_{41}NO_3Si_2$) 1** (10 g, 21.5 mmol) were weighed in a three-necked round bottom flask, triethylamine (1.2 eq., 25.82 mmol) was added and the mixture was fully dissolved in methanol (1 mmol cm^{-3} of the combined molecules). The solution was stirred and cooled to 0 °C in an ice bath. Consequently, acryloyl chloride (2 eq., 43.04 mmol) was dissolved in tetrahydrofuran (2 mmol cm^{-3}), triethylamine (1.2 eq. to acryloyl chloride, 51.65 mmol) were dissolved in methanol (4 mmol cm^{-3}) and simultaneously added dropwise to the cold solution. The reaction was slowly allowed to warm up to room temperature and the solvent was removed under vacuum. The residue was taken up in dichloromethane and extracted twice with 1% hydrochloric solution and once with brine. The organic layer was dried over sodium sulfate, the solvent was removed under reduced pressure and the product was used for polymerization without further purification. Yield: 9.97 g of light orange solid (90% purity = > 95.4% yield of **2**); HRMS: m/z calculated for $[C_{23}H_{42}NO_3Si_2]^+$ ($[M+H]^+$) 436.2698, found 436.2697; ^{1}H NMR (300 MHz, $CDCl_3$): δ = 6.76 (1H, d, J = 7.9, Ar–**H**), 6.68–6.55 (2H, m, Ar–**H**), 6.24 (1H, dd, J = 17.0, 1.6 Hz, NH–(C = O)–C**H**–CH_2), 6.01 (1H, dd, J = 17.0, 10.2 Hz, NH–(C = O)–CH–**H$_2$**), 5.60 (1H, dd, J = 10.2, 1.6 Hz, NH–(C = O)–CH–C**H$_2$**), 3.53 (2H, q, Ar–C**H$_2$**–CH_2–NH), 2.72 (2H, t, J = 6.9 Hz, Ar–CH_2–C**H$_2$**–NH), 0.98 (18H, br, Si–C–(C**H$_3$**)$_3$), 0.18 (12H, d, J = 1.7 Hz, Si–(C**H$_3$**)$_2$) ppm; ^{13}C NMR (75 MHz, $CDCl_3$): δ = 165.4,

146.8, 145.6, 131.7, 130.9, 126.3, 121.6, 121.5, 121.1, 40.7, 34.8, 25.9, 18.4, − 4.0, − 4.1 ppm.

***N*-(2-Phenylethyl)acrylamide (3, $C_{11}H_{13}NO$)** In analogy to the synthesis of **2**. Phenethylamine (10 g, 82.5 mmol) and triethylamine (1.2 eq.; 99.02 mmol) were dissolved in methanol (1 mmol cm^{-3} of the combined molecules). The solution was stirred and cooled to 0 °C in an ice bath. Consequently, acryloyl chloride (2 eq., 165.04 mmol) was dissolved in tetrahydrofuran (2 mmol cm^{-3}), triethylamine (1.2 eq. to acryloyl chloride, 198.05 mmol) were dissolved in methanol (4 mmol cm^{-3}) and simultaneously added dropwise to the cold solution. The reaction was slowly allowed to warm up to room temperature and the solvent was removed under vacuum. The residue was taken up in dichloromethane and extracted twice with 1% hydrochloric solution and once with brine. The organic layer was dried over sodium sulfate, the solvent was removed under reduced pressure and the product was used for polymerization without further purification. Yield: 14.22 g of light yellow oil (90% purity = > 88.5% yield of **3**); ^{1}H NMR (300 MHz, $CDCl_3$): δ = 7.38–7.13 (5H, m, Ar–**H**), 6.24 (1H, dd, J = 17.0, 1.6 Hz, NH–(C = O)–C**H**–CH_2), 6.06 (1H, dd, J = 17.0, 10.1 Hz, NH–(C = O)–CH–C**H**$_2$), 5.60 (1H, dd, J = 10.2, 1.7 Hz, NH–(C = O)–CH–C**H**$_2$), 3.58 (2H, q, J = 5.9 Hz, Ar–C**H**$_2$–CH_2–NH), 2.85 (2H, t, J = 7.1 Hz, Ar–CH_2–C**H**$_2$–NH) ppm.

Polymer synthesis

Unless stated otherwise, all polymers were synthesized in benzene at reflux temperature under argon atmosphere. The solvent was bubbled with nitrogen for at least 20 min. prior to use to remove radical-quenching oxygen. As initiator, 2 mol% in relation to all combined co-monomers of AIBN were used and if not defined differently, the reactions were quenched by removing from heat after 4 h.

Butyl acrylate co-polymers (P(BA–TDAXX))

Acrylamide **2** was weighed in a two-necked round bottom flask, AIBN was added in dry state and both molecules were consequently dissolved in the solvent. The two-necked round bottom flask was connected to a reflux cooler, solvent was added and the whole setup was flushed with argon gas. Butyl acrylate was added via a septum and the mixture was homogenized for 5 min. prior to heating to 80 °C. After 4 h the mixture was further concentrated, taken up in a syringe and precipitated in cold methanol twice. Polymers with 1, 10, 20, and 30% amount of **2** were produced and are named P(BA–TDA1), P(BA–TDA10), P(BA–TDA20), and P(BA–TDA30), respectively. Yield ranged between 50% and up to 92% of colorless/light yellow polymer. Depending on the amount of butyl acrylate, polymers were more (higher amount) or less (lower amount) oily. P(BA–TDA20): ^{1}H NMR (300 MHz, $CDCl_3$): δ = 6.74–6.65 (0.3H), 4.03 (2H), 3.35 (0.2H), 2.64 (0.2H), 2.28 (1H), 1.59 (2.6H), 1.36 (2.1H), 1.00–0.87 (4.6H), 0.17 (1H) ppm; T_g = − 35 °C (P(BA–TDA1)), − 27 °C (P(BA–TDA10)), − 14 °C (P(BA–TDA20)), 3 °C (P(BA–TDA30)).

Methyl acrylate co-polymers (P(MA–TDAXX))

The procedure was performed similarly to butyl acrylate-based polymers. Polymers with 20 and 30% amount of **2** were produced, and are named P(MA–TDA20) and P(MA–TDA30), respectively. Yield ranged between 64% and up to 92% of light yellow solid material. P(MA–TDA30): ^{1}H NMR (300 MHz, $CDCl_3$): δ = 6.74–6.66 (0.9H), 6.03 (0.2H), 3.65 (3H), 3.38 (1.3H), 2.65 (0.8H), 2.31 (1.9H), 1.93 (1.5H), 1.62 (1.7H), 1.49 (1.7H), 1.25 (0.2H), 0.97 (5.4H), 0.18 (2.3H) ppm.

Co-polymers of 2 and 3 (P(PAA–TDAXX))

The procedure was performed similarly to butyl acrylate-based polymers. Polymers with 10 and 20% of **2** were produced and are named P(PAA–TDA10) and P(PAA–TDA20), respectively. Yield ranged from 80 to 92% of light yellow solid material. P(PAA–TDA10): ^{1}H NMR (300 MHz, $CDCl_3$): δ = 7.13 (5.5H), 6.62 (1.5H), 3.35 (4H), 2.72 (4H), 1.77 (1.2H), 1.63 (7.2H), 1.25 (0.4H), 0.94 (5.1H), 0.15 (2.5H) ppm; T_g = 85 °C (P(PAA–TDA10)), 95 °C (P(PAA–TDA20)).

Butyl acrylate co-polymers without the catechol moiety (P(BA-PAA20))

Procedure was performed similarly to butyl acrylate-based polymers. Yield ranged from 60 to 80% of white honey-like material. ^{1}H NMR (300 MHz, $CDCl_3$): δ = 7.34–7.16 (1H), 4.02 (2H), 3.45 (0.5H), 2.79 (0.4H), 2.28 (1H), 1.90 (0.5H), 1.59 (0.9H), 1.36 (2.2H), 0.93 (2.6H) ppm; T_g = − 23 °C.

Homopolymer of 3 (P(PAA))

Procedure was performed similarly to butyl acrylate-based polymers. Yield ranged from 80 to 90% of light yellow solid. ^{1}H NMR (300 MHz, $CDCl_3$): δ = 7.13 (5H), 5.99 (1H), 3.36 (3H), 2.72 (3H), 2.40 (0.7H), 1.90–1.26 (3.6H) ppm; T_g = 80 °C.

Deprotection of TBS-protecting groups

All deprotections were performed in THF at a concentration of 250 mg cm^{-3}. TBAF was added as a 1 M solution under argon atmosphere and the mixture was stirred for 30 min at room temperature. After the reaction is finished, the

solution is taken up in a syringe and precipitated in a cold MeOH:H_2O (2:1) mixture which was acidified to pH < 2. Yields were between 80 and 90%. All polymer lost the T in the nomenclature, indicating the loss of the protecting group (P(BA–TDAXX)—> P(BA–DAXX) and so on).

Supplementary Information The online version contains supplementary material available at https://doi.org/10.1007/s00706-023-03057-4.

Acknowledgements The Comet Centre CEST is funded within the framework of COMET – Competence Centers for Excellent Technologies by BMVIT, BMDW as well as the Province of Lower Austria and Upper Austria. The COMET program is run by FFG. This work originates from research in DuraBond (FFG 865864 CEST-K1). The authors gratefully acknowledge Assoc. Prof. Dr. Clemens Schwarzinger for assistance with HRMS measurements. A special thank-you to Karl Schütz for his support in field experiments of adhesion test (see graphical abstract) and production of the stamps for tensile testing. The NMR spectrometer was acquired in collaboration with the University of South Bohemia (CZ) with financial support from the European Union through the EFRE INTERREG IV ETC-AT-CZ program (project M00146, "RERI-uasb").

Funding Open access funding provided by Johannes Kepler University Linz.

Data availability The authors declare that the data supporting the findings of this study are available within the paper and its Supplementary Information files. Should any raw data files be needed in another format they are available from the corresponding author upon reasonable request.

References

1. Amini S, Kolle S, Petrone L, Ahanotu O, Sunny S, Sutanto CN, Hoon S, Cohen L, Weaver JC, Aizenberg J, Vogel N, Miserez A (2017) Science 357:668
2. Ahn BK, Das S, Linstadt R, Kaufman Y, Martinez-Rodriguez NR, Mirshafian R, Kesselman E, Talmon Y, Lipshutz BH, Israelachvili JN, Waite JH (2015) Nat Commun 6:8663
3. Sever MJ, Weisser JT, Monahan J, Srinivasan S, Wilker JJ (2004) Angew Chem Int Ed 43:448
4. Waite JH (2017) J Exp Biol 220:517
5. Hwang DS, Zeng H, Masic A, Harrington MJ, Israelachvili JN, Waite JH (2010) J Biol Chem 285:25850
6. Harrington MJ, Jehle F, Priemel T (2018) Biotechnol J 13:e1800133
7. Li Y, Cheng J, Delparastan P, Wang H, Sigg SJ, DeFrates KG, Cao Y, Messersmith PB (2020) Nat Commun 11:3895
8. Li Y, Wang T, Xia L, Wang L, Qin M, Li Y, Wang W, Cao Y (2017) J Mater Chem B 5:4416
9. Hong S, Lee H, Lee H (2014) Beilstein J Nanotechnol 5:887
10. Wang Y, Park JP, Hong SH, Lee H (2016) Adv Mater 28:9961
11. Lopez-Perez PM, da Silva RMP, Strehin I, Kouwer PHJ, Leeuwenburgh SCG, Messersmith PB (2017) Macromolecules 50:8698
12. Wirthl D, Pichler R, Drack M, Kettlguber G, Moser R, Gerstmayr R, Hartmann F, Bradt E, Kaltseis R, Siket CM, Schausberger SE, Hild S, Bauer S, Kaltenbrunner M (2017) Sci Adv 3:e1700053
13. Shin M, Park S-G, Oh B-C, Kim K, Jo S, Lee MS, Oh SS, Hong S-H, Shin E-C, Kim K-S, Kang S-W, Lee H (2017) Nat Mater 16:147
14. Kastrup CJ, Nahrendorf M, Figueiredo JL, Lee H, Kambhampati S, Lee T, Cho S-W, Gorbatov R, Iwamoto Y, Dang TT, Dutta P, Yeon JH, Cheng H, Pritchard CD, Vegas AJ, Siegel CD, MacDougall S, Okonkwo M, Thai A, Stone JR, Coury AJ, Weissleder R, Langer R, Anderson DG (2012) Proc Natl Acad Sci 109:21444
15. Tiu BDB, Delparastan P, Ney MR, Gerst M, Messersmith PB (2019) ACS Appl Mater Interfaces 11:28296
16. Forg S, Karbacher A, Ye Z, Guo X, von Klitzing R (2022) Langmuir 38:5275
17. Quan-Li L, Qing-qing W, Xiaopeng Z, Yuan-Cong Z (2021) J Adhes Sci Technol 35:2410
18. Xiong X, Liu Y, Shi F, Zhang G, Weng J, Qu S (2018) J Bionic Eng 15:461
19. Grassie N, Torrance B, Fortune JD, Gemmell JD (1965) Polymer 6:653
20. Jenkins CL, Meredith HJ, Wilker JJ (2013) ACS Appl Mater Interfaces 5:5091
21. Boulding NA, Millican JM, Hutchings LR (2019) Polym Chem 10:5665
22. Jyothi TM, Raja T, Talawar MB, Rao BS (2001) Appl Catal A 211:41
23. Knaggs S, Malkin H, Osborn HMI, Williams NAO, Yaqoob P (2005) Org Biomol Chem 3:4002
24. Higginson CJ, Malollari KG, Xu Y, Kelleghan AV, Ricapito NG, Messersmith PB (2019) Angew Chem Int Ed 58:12271
25. Tsutsumi K, Tsukahara Y, Okamoto Y (1994) Polym J 26:13
26. Edeleva M, Marien YW, Van Steenberge PHM, D'hooge DR (2021) Polym Chem 12:2095
27. Zhang X, Liu H, Yue L, Bai Y, He J (2020) J Mater Sci 55:7981
28. Jakubowski W, Juhari A, Best A, Koynov K, Pakula T, Matyjaszewski K (2008) Polymer 49:1567
29. Banea MD, de Sousa FSM, Da Silva LFM, Campilho RDSG, de Pereira AMB (2011) J Adhes Sci Technol 25:2461
30. Penzel E, Ballard N, Asua JM (2010) Ullmann's encyclopedia of industrial chemistry, 7th edn. Wiley-VCH Wiley online library, Weinheim
31. Lee BP, Dalsin JL, Messersmith PB (2002) Biomacromol 3:1038
32. Charlot A, Sciannaméa V, Lenoir S, Faure E, Jérôme R, Jérôme C, van de Weerdt C, Martial J, Archambeau C, Willet N, Duwez A-S, Fustin C-A, Detrembleur C (2009) J Mater Chem 19:4117
33. Xu H, Nishida J, Wu H, Higaki Y, Otsuka H, Ohta N, Takahara A (2013) Soft Matter 9:1967
34. Yeon DK, Ko S, Jeong S, Hong S-P, Kang SM, Cho WK (2019) Langmuir 35:1227
35. White JD, Wilker JJ (2011) Macromolecules 44:5085
36. Jenkins CL, Siebert HM, Wilker JJ (2017) Macromolecules 50:561
37. Mu Y, Wu X, Pei D, Wu Z, Zhang C, Zhou D, Wan X (2017) ACS Biomater Sci Eng 3:3133
38. Jones TA, Wilker JJ (2020) ACS Appl Polym Mater 2:4632
39. Kester DR, Duedall IW, Connors DN, Pytkowicz RM (1967) Limnol Oceanogr 12:176